AIP Journal of Applied Physics

CL study of blue and UV emissions in β-Ga2O3 nanowires grown by thermal evaporation of GaN

G. Guzmán-Navarro, M. Herrera-Zaldívar, J. Valenzuela-Benavides, and D. Maestre

Citation: Journal of Applied Physics **110**, 034315 (2011); doi: 10.1063/1.3620986
View online: http://dx.doi.org/10.1063/1.3620986
View Table of Contents: http://scitation.aip.org/content/aip/journal/jap/110/3?ver=pdfcov
Published by the AIP Publishing

CL study of blue and UV emissions in β-Ga_2O_3 nanowires grown by thermal evaporation of GaN

G. Guzmán-Navarro,[1] M. Herrera-Zaldívar,[1,a)] J. Valenzuela-Benavides,[1] and D. Maestre[2]
[1]*Centro de Nanociencias y Nanotecnología, Universidad Nacional Autónoma de México, Ensenada, Baja California 22800, México*
[2]*Departamento de Física de Materiales, Universidad Complutense de Madrid, Madrid 28040, Spain*

(Received 19 March 2011; accepted 30 June 2011; published online 12 August 2011)

We report a cathodoluminescence (CL) study of β-Ga_2O_3 nanowires grown by thermal evaporation of GaN on Si(100) and Au/Si(00) substrates. Condensation and subsequent oxidation of metallic Ga is suggested as the growth mechanism of β-Ga_2O_3 nanowires. The β-Ga_2O_3 nanowires grown on Si(100) show multiple bends or undulations, together with a strong UV emission at 3.31 eV and a weak blue emission centered at 2.8 eV as a band component. The β-Ga_2O_3 nanowires grown on Au/Si(100) substrates recorded a lower CL intensity of a well-defined blue emission of 2.8 eV. A thermal treatment on these samples produced an increase of the UV emission and quenching of the blue band. Thermal annealing of oxygen vacancies is proposed as the responsible mechanism for the observed behavior of these samples. © *2011 American Institute of Physics*. [doi:10.1063/1.3620986]

I. INTRODUCTION

The monoclinic gallium oxide (β-Ga_2O_3) is a semiconductor with a wide bandgap of about 4.9 eV with potential applications in optoelectronics such as waveguides and optical emitters for UV radiation,[1,2] gas sensing,[3] and photocatalysis.[4] As other semiconductor nanostructures, the β-Ga_2O_3 has received special attention for its improved luminescent properties due to quantum confinement effects. These properties would allow the design of light emitters with high quantum efficiency. Many efforts have been devoted to optimize the synthesis of this semiconductor and achieve control of its luminescent properties. Particularly, the growth of β-Ga_2O_3 nanowires has been reported by thermal evaporation,[5] arc-discharge,[6] the hydrothermal method, and metal-organic chemical vapor deposition (MOCVD).[7,8] However, β-Ga_2O_3 has shown undesired emissions due to the presence of impurities or point defects generated by still unclear mechanisms that must be elucidated. Perhaps the most well-known defect related emission attributed to oxygen vacancies is the blue band centered between 2.6 and 2.9 eV, with a relative peak intensity dependent on the growth method used.[9]

Cathodoluminescence (CL) is a widely used technique for semiconductor characterization because its high sensitivity to detect changes in luminescence produced by impurities and point defects. In this article, we present a CL study of the generation of point defects in β-Ga_2O_3 nanowires grown on Si(100) and Au/Si(100) substrates by thermal decomposition of GaN with different carrier gases and low pressure. We discuss the effect of the growth conditions and thermal annealing on the defect structure in β-Ga_2O_3 nanowires.

a)Author to whom correspondence should be addressed. Electronic mail: zaldivar@cnyn.unam.mx.

II. EXPERIMENTS

β-Ga_2O_3 nanowires were synthesized by thermal decomposition of GaN powder (AlfaAesar, 99.99%) onto oxidized Si(100) or gold coated (30-40 nm thick) Si(100) substrates. Samples were grown in a furnace built in our laboratory, operated at 100 mTorr when N_2 or Ar was used as carrier gases (Infra, 99.998%), or 0.1 mTorr when no carrier gas was used. A mechanical pump maintained the desired pressure of the system. The gas flow was regulated by a needle valve and monitored by a mass flow meter (Omega type FMA-A2302). The GaN powder was placed on an alumina boat at the center of the furnace and held at a temperature of 1500 °C to be evaporated. The carrier gas and the vacuum pumping flow transported the GaN vapor to the substrates. A linear manipulator equipped with a K-type thermocouple allowed the control of the growth temperature by placing the substrates at different positions at the downstream end of the tube furnace. Samples 1 and 2 were grown on Si(100) substrates at 250 and 360 °C, respectively, with different carrier gas. Sample 1 was grown with a 7.8 sccm Ar flow rate for 4 hr, while sample 2 was grown with 30 sccm N_2 flow rate for 8 hr. Samples 3 and 4 were grown on Au/Si(100) substrates at 350 °C and 300 °C, respectively, for 6 hr without carrier gas at 10^{-4} Torr, and subsequent annealing at 750 °C in high vacuum (10^{-4} Torr) for 1 hr.

For structural characterization, a Phillips X'pert x-ray diffractometer with a CuK_α ($\lambda = 0.154$ nm) line excitation source was used. Morphology and elemental composition were evaluated by SEM using a Jeol JSM-5300 and a Bruker analytical system, respectively. For HRTEM measurements, a Jeol JEM 2010 operated at 200 keV was used to determinate the growth direction and crystallinity of nanowires. CL measurements were performed in an SEM at room and low temperature (90 K) in the UV-visible spectral range with electron beam energy of 15 keV. A Hamamatsu R928P

photomultiplier tube and a SPEX 340E monochromator were used for spectral analysis.

III. RESULTS AND DISCUSSION

XRD measurements revealed a crystalline structure of samples corresponding to monoclinic β-Ga_2O_3. Figures 1(a) to (c) show XRD spectra from samples 1-3, respectively, with high intensity from the (-202), (111), (-113), and (-217) peaks in all samples, which reveal similar crystalline characteristics between nanowires.

SEM images from sample 1 show the presence of scepter type structures, composed by spheres with diameters between 1 and 15 μm attached to wires with diameters between 100 nm and 1 μm (Fig. 2(a)). The larger spheres showed the unexpected behavior of collapsing in high vacuum when the sample was cooled down to 90 K (inset in Fig. 2(a)), recovering their spherical shape after heating back to room temperature, leaving noticeable surface grooves (labels A and B in Fig. 2(a)). This behavior suggests that spheres are hollow but filled with a gas. EDS measurements revealed that spheres are composed mainly of metallic gallium, while their tail part contains oxygen and gallium as the elemental mapping in Fig. 3 shows. Formation of Ga-rich solid spheres at the end of β-Ga_2O_3 nanowires grown by MOCVD was reported previously by Sacilotti *et al.*[8] The authors suggest that decomposition of the metal-organic precursor used in their synthesis formed Ga spheres, which in turn acted as catalyst in the growth of β-Ga_2O_3 nanowires. Moreover, the synthesis of β-Ga_2O_3 nanowires by thermal evaporation of metallic gallium, and their subsequent oxidation has been reported by several authors.[10–12] In our case, metallic gallium produced by decomposition of GaN apparently condenses on substrates and oxidizes by residual air, therefore allowing the growth of β-Ga_2O_3 nanowires. The thermal diffusion of condensed gallium droplets during their oxidation could explain the undulations of several β-Ga_2O_3 nanowires found in this sample (Fig. 5(a)).

Sample 2 shows longer nanowires that those found in sample 1 with diameters between 200 and 500 nm and with many bends along their length (Fig. 1(b)). As in sample 1, a small sphere appeared at the end of nanowires [inset in Fig. 1(b)], which suggest a similar growth mechanism for both samples. To gain insight into the crystal growth mechanism, HRTEM images were taken from different regions where a bend occurs (Fig. 4(a)). Region 1 shows a stacking fault that delimits the nanowire growth direction (Fig. 4(b)). Regions 2 and 3 show that before and after of the bend, the nanowire growth changed from the axial [100] direction to a direction with components along the [100] and [001] directions without modify their atomic alignment, which is typical of a slip plane growth (Figs. 4(c) and 4(d)). Region 3 also shows a jagged surface produced precisely by the anisotropic growth direction of the nanowire. Growth of β-Ga_2O_3 nanowires with symmetric twinning along the wire axis has been reported,[12] and there is speculation that this defect would explain a fast axial growth rate over the growth rate in the radial direction. We did not find evidence of the presence of symmetric twinning in our samples, a fact that may explain the characteristic bending of our structures.

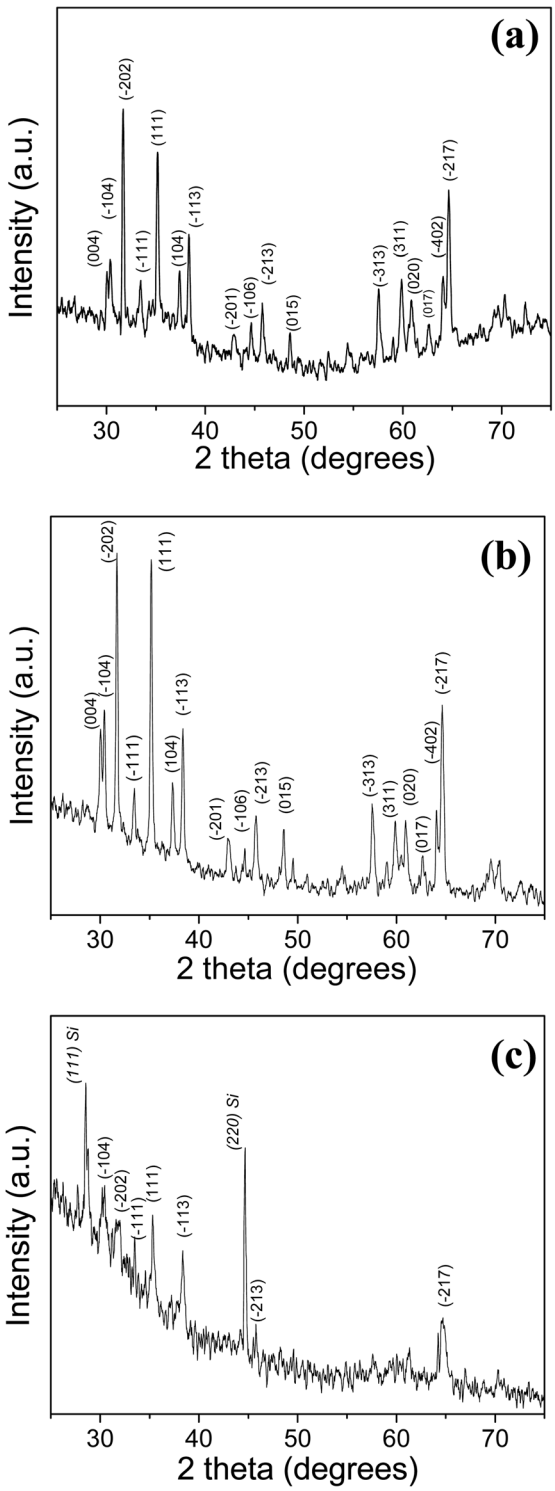

FIG. 1. XRD patterns from samples (a) to (c) 1-3 with peaks corresponding to β-Ga_2O_3.

Samples 3 and 4, grown on Au/Si(100), show a more homogeneous and thinner β-Ga_2O_3 nanowires when compared to the other two previous samples, with diameters between 120 and 80 nm (Figs. 2(c) and 2(d)), respectively, clearly the result of using Au catalyst.

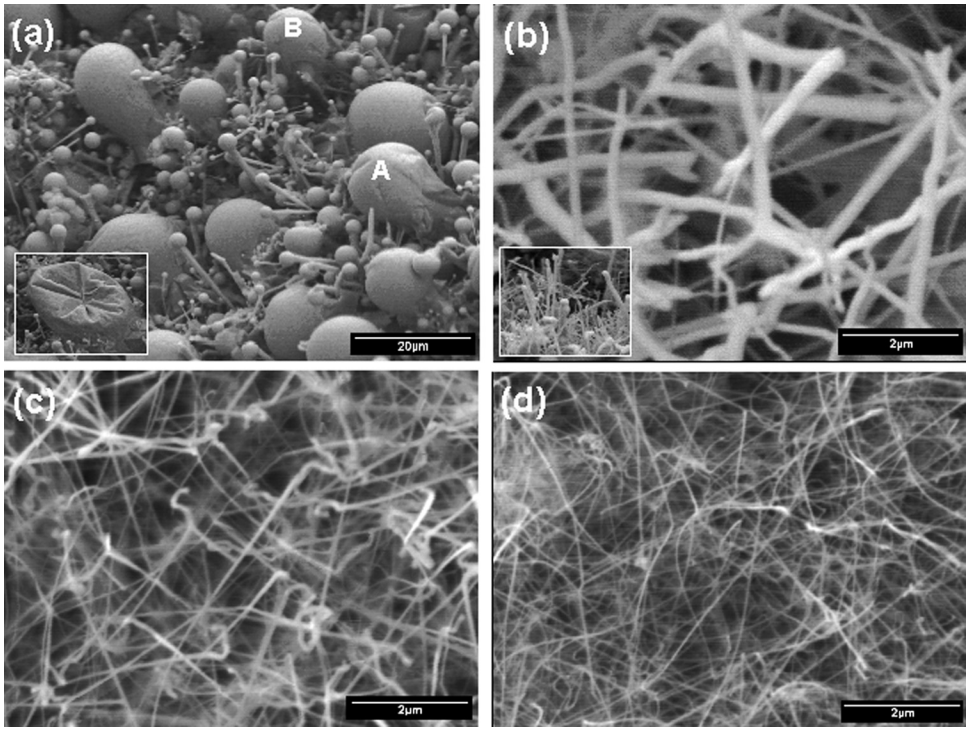

FIG. 2. Typical SEM images of β-Ga_2O_3 nanowires from (a) sample 1 with nanowires and hollow spheres (inset show a deflated sphere and labels A and B signing the groves produced after inflating), (b) sample 2 with bended nanowires with a sphere in their end (inset), and (c) and (d) samples 3 and 4, respectively, with regular thin nanowires.

CL images from sample 1 show luminescence originated from the tail of the sceptre-like structures, while their gallium head appears as a non-emitting dark sphere (Figs. 5(a) and (b)). Measurements at higher magnification show an inhomogeneous luminescence emission along the wires with bright and dark regions as the inset in Fig. 5(b) shows. CL images of β-Ga_2O_3 nanowires in sample 2 also show inhomogeneous luminescence with darker regions where bends are present (arrows in Figs. 5(c) and 5(d)). This effect can be attributed to the presence of nonradiative centers, such as stacking faults, as previously shown in Fig. 4(b). Finally, CL images from sample 3 (similarly for sample 4) revealed a more homogeneous luminescence of the thinner nanowires as show Fig. 5(f).

Figures 6(a) and 6(b) show CL normalized spectra acquired at 90 and 300 K from samples 1 and 2, respectively, with a broad UV emission centered at about 3.31 eV. The origin of this emission has been assigned to a recombination of

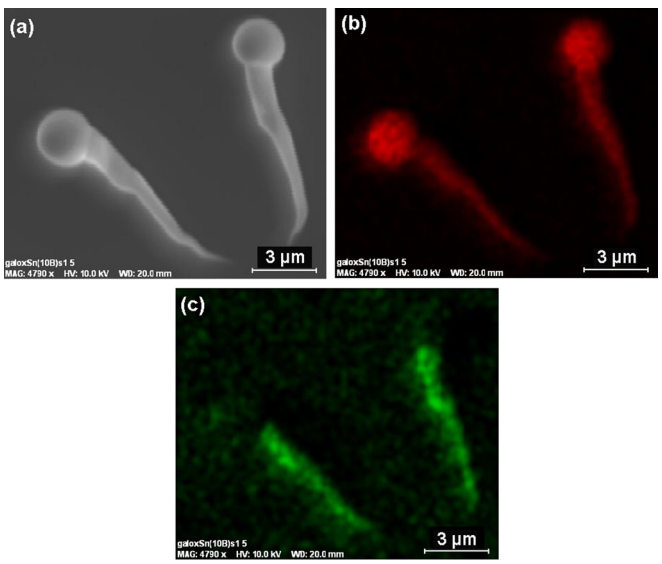

FIG. 3. (Color online) (a) SEM image and EDS elemental mapping for (b) gallium (K series) and (c) oxygen (K series) over the same area.

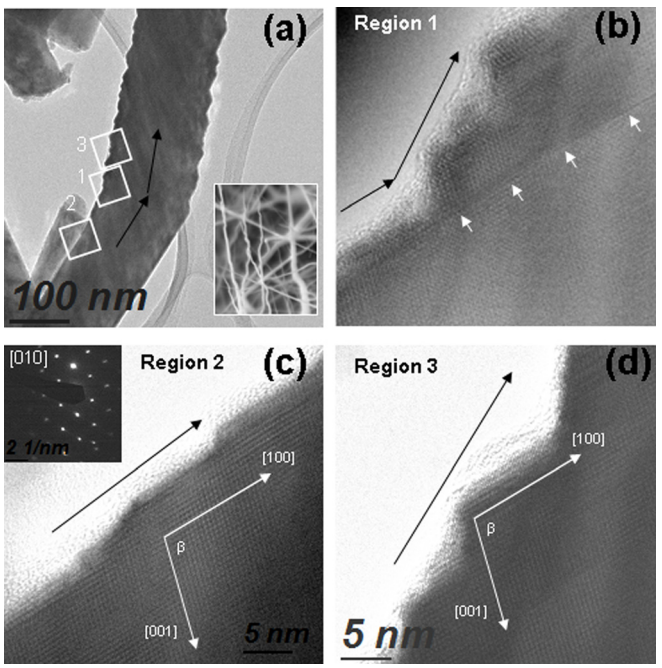

FIG. 4. (a) Typical TEM image of a β-Ga_2O_3 nanowire from sample 2 revealing a bend. Inset show a SEM image of nanowires with several bends. (b) HRTEM image of the bended nanowire from region 1 with a stacking fault (white arrows), (c) region 2 with growth along the [100] direction, and (d) region 3 with the same atomic alignment of region 2. Black arrows show the growth direction of the nanowire.

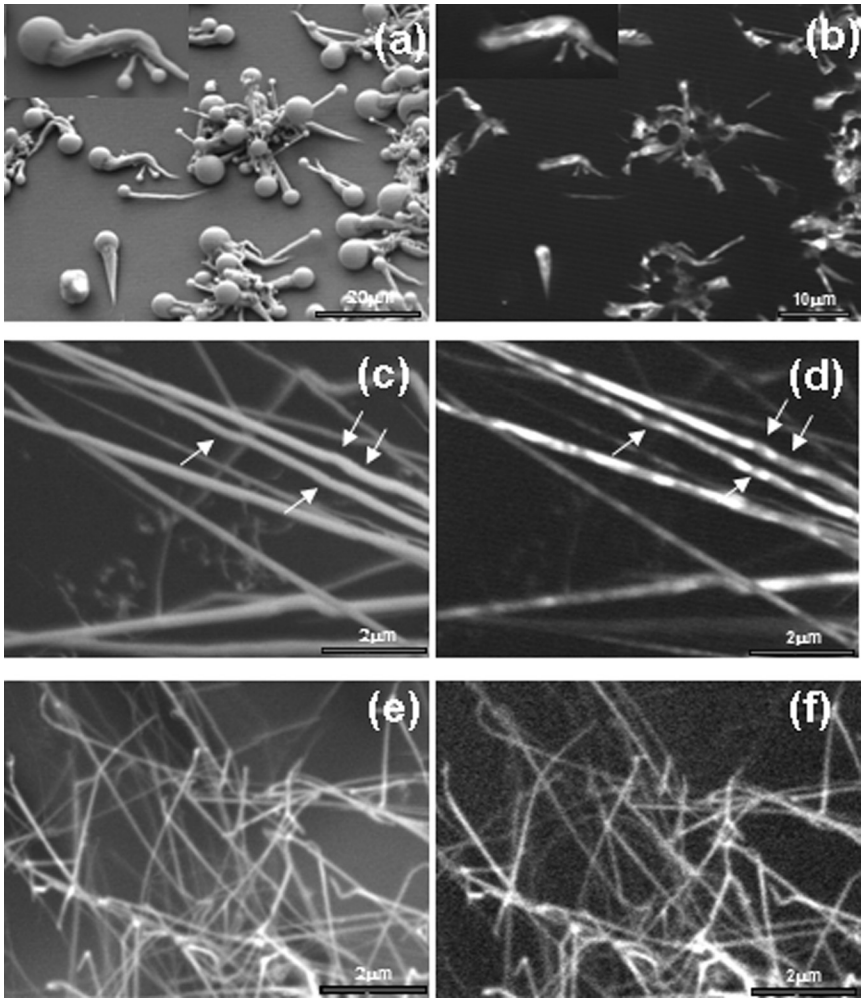

FIG. 5. Typical SEM images and their corresponding CL images of β-Ga_2O_3 nanowires for (a) and (b) sample 1, (c) and (d) sample 2, and (e) and (f) sample 3. The arrows show bends in the nanowires of sample 2.

self-trapped excitons by several authors,[9,13,14] apparently with an intensity dependence on doping and growth conditions.[13] As Figs. 6(a) and 6(b) show, the 300 K spectrum of sample 2 is slightly broader toward the low energy end than spectrum of sample 1 acquired at the same temperature, with FWHM values of 0.62 and 0.59 eV, respectively. We have assigned this slight difference to the presence of a blue component in the emission of sample 2, centered at about 2.8 eV as the deconvoluted Gaussian curve in Fig. 6(e) reveals.

CL spectra from samples grown on Au/Si(100) substrates recorded an overall lower CL intensity at 300 K with a clear presence of a blue emission at 2.8 eV (Figs. 6(c) and 6(d)). The deconvoluted CL spectrum of sample 3 acquired at 300 K reveals that the blue emission dominates over the UV emission (Fig. 6(f)), an effect that is more pronounced in sample 4 at the same temperature and before the annealing treatment. The β-Ga_2O_3 blue emission has been reported by several authors[7,15,16] and has been attributed to a donor-acceptor transition, between neutral oxygen vacancies (V_O^x) as donor, and oxygen-gallium vacancies pair (V_O, V_{Ga}) as acceptor.[9,13] CL spectra acquired at 90 K from samples 3 and 4 show a blue-shift of 150 meV and 470 meV, respectively (Figs. 6(c) and 6(d)). This effect is explained in terms of a relative intensity decrease (increase) of the blue (UV) band. Similar behavior has been found by Harwig *et al.* in pure and doped β-Ga_2O_3 crystals, revealing that for temperatures above 120 K, the blue emission is often observed in addition to the UV emission.[14] These authors suggest that UV emission is intrinsic and that impurities or the history of the samples neither influence its intensity nor its energy and conclude by assigning its origin to a recombination between an electron (hole) and a self-trapped hole (electron). A noticeable effect in our last two samples is the strong quenching of the blue emission band after annealing at 750 °C (Figs. 6(c) and 6(d)). As the CL spectra show, only the UV band centered at 3.28 eV is present with a FWHM of about 0.55 eV for both samples. This quenching of the blue emission is a strong indicator that thermal treatment eliminated most of the point defects responsible of this emission. Similar behavior was found by Nogales *et al.* in thermally treated β-Ga_2O_3 nanowires at 1500 °C for 24 hr, noticing an increase in intensity of the UV band.[16] As has been indicated, oxygen vacancies produce donor and complex-acceptor centers responsible for the β-Ga_2O_3 blue emission. Shimamura *et al.* recently proposed that a decrease of the relative intensity of the blue emission is due to the decrease in the number of oxygen vacancies.[13] We propose that the annealing treatment of samples 3 and 4 greatly eliminated oxygen vacancies, and because this

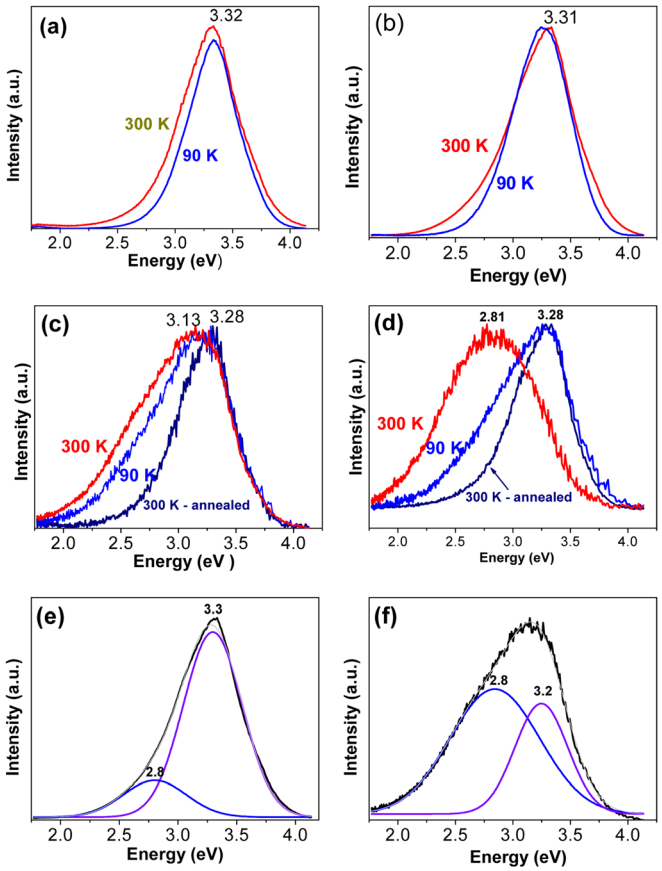

FIG. 6. (Color online) Normalized CL spectra acquired at 90 and 300 K from (a) to (d) samples 1 - 4, respectively. Deconvoluted CL spectrum acquired at 300 K from the (e) sample 1 and (f) the sample 3.

treatment was performed in high vacuum, we suggest that oxygen vacancies annealed in our samples by a thermal diffusion process.

IV. CONCLUSIONS

We report a cathodoluminescence (CL) study in β-Ga_2O_3 nanowires grown on Si(100) and Au/Si(00) substrates by thermal evaporation of GaN. Condensation and subsequent oxidation of metallic Ga is suggested as the growth mechanism of β-Ga_2O_3 nanowires. The β-Ga_2O_3 nanowires grown on Si(100) show bends or undulations, while nanowires grown on Au/Si(100) substrates are thinner and homogeneous. HRTEM measurements show formation of stacking faults that delineate the characteristic nanowire morphology and growth direction. A strong UV emission at 3.31 eV was recorded from samples grown on Si(100) with a weak blue emission centered at 2.8 eV as a band component. The β-Ga_2O_3 nanowires grown on Au/Si(100) show an overall lower CL intensity with a well-defined blue emission at 2.8 eV. A thermal treatment of the samples increased the UV emission and quenched the blue band. Annealing of oxygen vacancies is proposed as the mechanism responsible for this behavior.

ACKNOWLEDGMENTS

This work was partially supported by grants from CONACyT (Grant No. 102519) and PAPIIT-UNAM (Grant No. IN102111), Mexico. Technical help from E. Aparicio, E. Flores, F. Ruiz, A. Tiznado, I. Gradilla, D. Domínguez, and L. Gradilla is greatly appreciated.

[1]E. Nogales, J. A. García, B. Méndez, and J. Piqueras, J. Appl. Phys. **101**, 033517 (2007).
[2]E. Nogales, J. A. García, B. Méndez, and J. Piqueras, Appl. Phys. Letts. **91**, 133108 (2007).
[3]M. Ogita, N. Saika, Y. Nakanishi, and Y. Hatanaka, Appl. Surf. Sci. **142**, 188 (1999).
[4]Y. D. Hou, X. C. Wang, L. Wu, Z. X. Ding, and X. Z. Fu, Environ. Sci. Technol. **40**, 5799 (2006).
[5]B. C. Kim, K. T. Sun, K. S. Park, K. J. Im, T. Noh, M. Y. Sung, S. Kim, S. Nahm, Y. N. Choi, and S. S. Park, Appl. Phys. Lett. **80**, 479 (2002).
[6]P. Gyeong-Su, Ch. Won-Bong, K. Jong-Min, Ch. Young-Chul, L. Young-Hee, and L. Chang-Bin, J. Crystal Growth **220**, 494 (2000).
[7]Y. Quan, D. Fang, X. Zhang, S. Liu, and K. Huang, Mater. Chem. Phys. **121**, 142 (2010).
[8]M. Sacilotti, P. Cheyssac, G. Patriarche, J. Decobert, Th. Chiaramonte, L. P. Cardoso, M. F. Pillis, M. J. Brasil, F. Iikawa, M. Nadaema, Y. Lacroute, J. C. Vial, and F. Donatini, Surf. Coat. Technol. **201**, 9104 (2007).
[9]L. Binet and D. Gourier, J. Phys. Chem. Solids **59**, 1241 (1998).
[10]K. Hong Choi, K. Koo Cho, G. Bong Cho, H. Jun Ahn, and K. Won Kim, J. Crystal Growth **311**, 1195 (2009).
[11]C. Li-Wei, Y. Jien-Wei, L. Ching-Fei, H. Meng-Wen, and C. S. Han, Thin Solid Films **518**, 1434 (2009).
[12]H. Z. Zhang, Y. C. Kong, Y. Z. Wang, X. Du, Z. G. Bai, J. J. Wang, D. P. Yu, Y. Ding, Q. L. Hang, and S. Q. Feng, Solid State Commun. **109**, 677 (1999).
[13]K. Shimamura, E. G. Víllora, T. Ujiie, and K. Aoki, Appl. Phys. Lett. **92**, 201914 (2008).
[14]T. Harwig, F. Kellendonk, and S. Slappendel, J. Phys. Chem. Solids **39**, 675 (1978).
[15]E. Nogales, B. Sánchez, B. Méndez, and J. Piqueras, Superlattices Microstruct. **45**, 156 (2009).
[16]E. Nogales, B. Méndez, and J. Piqueras, Appl. Phys. Lett. **86**, 113112 (2005).